# Single-phase bimetallic system for the selective oxidation of glycerol to glycerate†

**Di Wang,[a] Alberto Villa,[b] Francesca Porta,[b] Dangsheng Su[a] and Laura Prati*[b]**

*Received (in Cambridge, UK) 20th December 2005, Accepted 13th March 2006*
*First published as an Advance Article on the web 22nd March 2006*
**DOI: 10.1039/b518069d**

**Single phase bimetallic Au/Pd catalyst was prepared and characterised by TEM techniques. The high activity in the selective liquid phase oxidation of glycerol towards glycerate is unambiguously attributed to the synergistic effect of alloy.**

Recently, supported gold nanoparticles have attracted more and more interest due to their special activity in catalytic reactions.[1–8] In many cases, bimetallic systems like Au–Pd and Au–Pt show extra high activity and high resistance to deactivation due to synergistic effects.[9–13] However the system is often too complex to correlate the activity with the specific catalyst feature. Therefore the characterization of well-defined, highly active catalysts is essential. Some carefully designed surface systems have been successfully applied in test reactions to reveal the role of Pd or Au on catalyst surfaces.[14–16] The characterisation of metal surfaces is more difficult for nanoparticles, especially when the metal loading is very low.

In liquid phase applications, such as the oxidation of glycerol[17] (an important reaction for the industrial revaluation of this co-product in biodiesel manufacturing)[18] it has been reported that Pd/Au and Pt/Au nanoparticles supported on activated carbon (AC) show a strong synergistic effect.[10,11] Most syntheses provide a mixture of monometallic particles with bimetallic particles; no catalysts consisting of only single bimetallic-phase on carbon have been reported, making the design of catalysts a compulsory task for the understanding of the synergistic effect highlighted. Moreover, alloyed phases obtained by calcination present low metal dispersion. Metal segregation or multi-phases occur very often thus making the correlation between active species and catalytic performance very difficult or even speculative.[18,19]

In order to avoid any segregation of metal we used preformed particles of one metal as nucleation centres for the other metal. Thus we first immobilised a preformed gold sol (using $BH_4^-$ as reducing agent) on activated carbon, and then the sol of palladium was generated in the presence of Au/AC using $H_2$ as a second reducing agent instead of $NaBH_4$. Using $NaBH_4$ as reducing agent easily results in Pd segregation.[10] Slowing down the reduction rate of the palladium salt is the key to avoiding Pd segregation or homogenous nucleation that results in a mixture of monometallic phase and alloy.[10] The total metal loading was 1%wt. The electron micrograph of this catalyst (1%wt Pd@Au/AC) (Fig. 1) shows that the nanoparticles are evenly distributed on the activated carbon. The histogram of particle size distribution is inserted in Fig. 1. Most particles are smaller than 10 nm in size. The size distribution can be fitted approximately by a Gaussian function, which centred at 3.4 nm. In addition, only about 2% of particles have sizes from 10 nm up to 30 nm.

High-resolution imaging was performed on particles of different sizes. Representatively, the HRTEM images of a small particle (about 3 nm in size) and a big one (about 9 nm in size) are shown in Fig. 2. The small particle in the image exhibits a twin boundary as indicated by the straight line. The fast Fourier transforms (FFT) of both sides of the twin boundary are also inserted. Two sets of reflections are visible in either FFT map. The lattice spacing calculated from the FFT map has the value of about 2.29 Å, between the Pd (111) plane (2.25 Å) and the Au (111) plane (2.35 Å), which implies the alloy state. However, the angle between the two sets of (111) planes in either FFT map is about 56° instead of about 71° for an fcc single crystal. We can prove that such special values of the angle can be produced by two overlapped fcc lattices with a twin boundary in between. That means, there are more twin boundaries than just the one visible in the image and

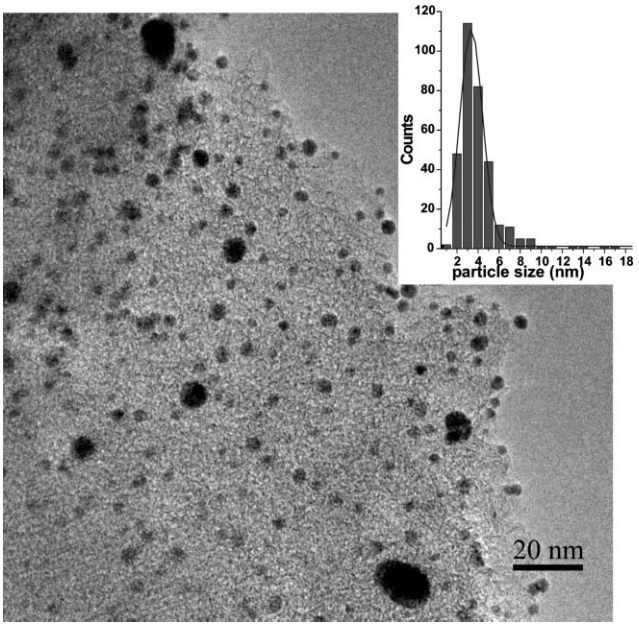


**Fig. 1** Overview TEM image of the 1% wt Pd@Au/C catalyst. The particle size distribution is shown in the inset.

[a]*Department of Inorganic Chemistry, Fritz Haber Institut der MPG, ELCASS, European Laboratory of Catalysis and Surface Science, Faradayweg 4-6, D-14195, Berlin, Germany*
[b]*Dipartimento di Chimica Inorganica Metallorganica e Analitica e ISTM, Centre of Excellence CIMAINA AURICAT Programme, Università di Milano, via Venezian 21, I-20133, Milano, Italy. E-mail: Laura.Prati@unimi.it; Fax: (+39) 02 503 14405*
† Electronic supplementary information (ESI) available: Detailed synthesis and experimental. See DOI: 10.1039/b518069d

 

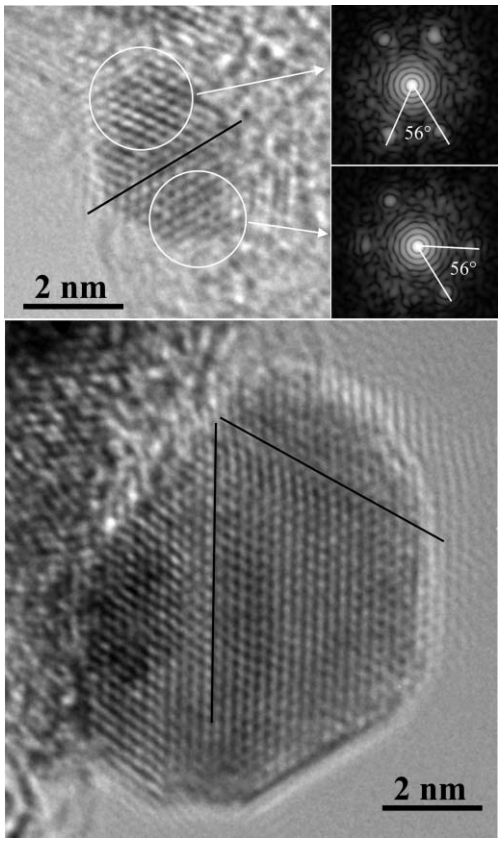


**Fig. 2** A small particle (about 3 nm in size) and a big one (about 9 nm in size), both showing multiply twinned structure. The twin boundaries in the images are indicated by straight lines. The FFTs of the two parts in the image of the small particle suggest additional twin boundaries, which are not directly visible. The HRTEM images show no structural incoherency.

this particle is a multiply twinned particle with each twinned part being fcc structure. The decahedron multiply twinned model fits our observation very well.[20] Metal particles with such multiply twinned structure are very common in colloidal chemistry and also observed in materials synthesized by chemical vapour deposition.[21,22] In the HRTEM image of the big particle (Fig. 2) two twin boundaries are visible. The measured lattice spacings and the angles in between are the same as those of the small particle, indicating the same multiply twinned structure. Most importantly, no core–shell structure or any structural incoherency was observed in the HRTEM images.

Since Au and Pd may form alloy at almost any ratio while keeping the fcc structure, it is essential to examine whether the metal compositions in individual particles coincide with "single-phase". With electron beam converged to the size of nanometers, X-ray photons emitted from the very local area can be detected in the microscope. By this way, EDX spectra were acquired from single particles and were compared with the overall spectrum. The single particle EDX acquisition was repeated on over fifty particles of different sizes. The overall spectrum and a representative one for individual single particles are shown in Fig. 3. The Au to Pd ratio obtained from this representative overall spectrum in Fig. 3 is 6.6 : 3.4. The ratios of Pd to Au are almost unchanged for all the examined single particles, regardless of the particle size, and are also similar to that of the overall measurement. This indicates that

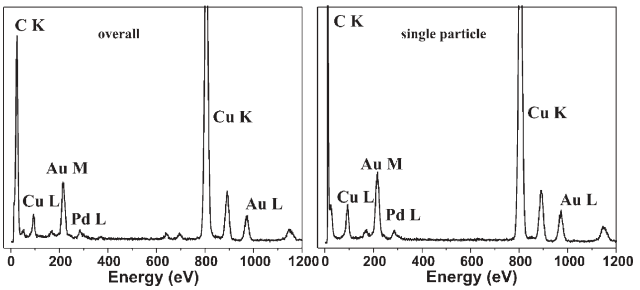


**Fig. 3** The overall EDX spectrum (left) and the representative spectra taken from an individual single particle (right). The Au–Pd ratio is similar for each particle. The strong Cu signals are from the Cu grid supporting the TEM samples.

the examined single particles are a good representative for the whole sample and there is no segregation of Pd or Au. In combination with the TEM observations, which show uniform structure within each particle, we can confirm that all the particles consist of random Au–Pd alloy, with the Au–Pd ratio close to 6 : 4. The XRD results are in good agreement with our TEM observations. For the present catalyst, XRD shows a broad peak at $2\theta$ of 39.0°, which corresponds to the lattice spacing of about 2.30 Å (2.29 Å measured by HRTEM). For the catalyst prepared as reported in ref. 10 (1%wt (Pd@Au)/AC), XRD with Rietveld analysis reveals 6 : 4 Au–Pd alloy and finely dispersed Pd.

Table 1 shows the results from the selective oxidation of glycerol. As expected the Pd/Au system reveals a significant synergistic effect compared with monometallic systems such as Pd/AC or Au/AC. Note that under given experimental conditions monometallic Pd deactivated before reaching high conversion, but at low conversion a good selectivity to glyceric acid was obtained ($S50$ = 80%).

For comparison we tested also the catalyst prepared as reported in ref. 10 (1%wt (Pd@Au)/AC) where bimetallic particles were generated in solution. The brackets in 1%wt(Pd@Au)/AC mean that the immobilisation step follows the generation of bimetallic particles. 1%wt(Pd@Au)/AC differs from 1% wt Pd@Au/AC only for the presence of segregated, highly dispersed Pd. The alloyed particle has the same (Au6Pd4) phase with similar dispersion. By comparing the activity of these two catalysts (Table 1), we observed that 1% wt Pd@Au/AC showed a significant increase of TOF (6435 *vs.* 4823 $h^{-1}$); the overall selectivity slightly increases (3%) compared with 1% wt (Pd@Au)/AC.

**Table 1** Selective oxidation of glycerol using 1%wt mono and 1%wt bimetallic catalysts at 50 °C[a]

| Catalyst | TOFmol (mol Au)$^{-1}$h$^{-1}$[b] | $S90$[c] | $D$/nm (TEM) |
|---|---|---|---|
| 1%Au/AC | 900 | 68 | 2.9 |
| 1%Pd/AC[d] | 1000 | 80[d] | 2.0 |
| 1%(Pd@Au)/AC | 4823 | 74 | 2.6 (alloy); < 2 (Pd) |
| 1%Pd@Au/AC | 6435 | 77 | 3.4 |

[a] Reaction conditions: water 10 ml, 0.3 M glycerol, glycerol/M = 3000, NaOH/glycerol = 4, $T$ = 50 °C, $pO_2$ = 3 atm. [b] Calculation of TOF (mol (mol Au)$^{-1}$h$^{-1}$) after 0.25 h of reaction. TOF numbers were calculated on the basis of total loading of metals by withdrawing and analyzing sample. [c] Selectivity to glyceric acid at 90% conversion. [d] This catalyst deactivates before reaching 90% conversion, selectivity is reported at 50% conversion.

Therefore, we can conclude that the alloyed phase is much more active than segregated palladium and that alloy is responsible for the high synergistic effect. The selectivity appears to be highly relevant to palladium as monometallic Pd showed an *S*50 similar to 1% wt Pd@Au/C (and also 1% wt (Pd@Au)/AC) whereas Au/AC showed a lower selectivity.

Thus, by using the two-step synthesis, we were able to obtain a single-phase Au6Pd4 catalyst (1% wt Pd@Au/AC), differing from another very similar catalyst only by a small amount of Pd segregation (1%wt (Pd@Au)/AC). The superior behaviour of the two bimetallic catalysts with respect to the monometallic ones and the direct comparison between the two systems led us to unambiguously attribute the high activity in the selective liquid phase oxidation of glycerol towards glycerate to the synergistic effect of alloy.

The characterization of the single-phase Au6Pd4 catalyst reveals that all the nanoparticles are random alloy with similar Au–Pd ratio. The lattice parameter of this alloy is between that of Au and that of Pd. Such modification causes change also in surface interatomic distances and therefore the electronic structure, even though there is no considerable electron transfer between Pd and Au.[23] Therefore the number of Pd or Au monomers on the bimetallic catalyst surfaces is greatly reduced.The highly improved activity could be attributed to the Au–Pd bifunctional sites. Such sites have been determined by HREELS to exist in a model catalyst at the edge of Au islands on the Pd (111) surface, responsible for CO "linear" adsorption.[16] Furthermore, it was found in acetoxylation of ethylene to vinyl acetate that Au acted as promoter to isolate Pd monomer sites, preventing undesirable pathways to CO, $CO_2$ and surface carbon.[15] The same mechanism could be responsible for avoiding deactivation, which is severe for the pure Pd catalyst. The strong base conditions were proposed to be essential in the initial abstraction of H from one of the primary hydroxyl groups of glycerol.[5,7] This condition has the same effect on the four catalysts presented in this paper.

In summary, a single-phase bimetallic catalyst supported on activated carbon is prepared in a two-step process by limiting the Pd species available through decreasing the reduction rate of the palladium salt. The single-phase Pd–Au catalyst exhibits higher performance in selective oxidation of glycerol than the monometallic Pd/AC, Au/AC and the mixed-phase Pd–Au catalyst. We confirm that the improved activity comes from the synergistic effect of alloy. The microstructures of the catalyst were characterised by HRTEM and EDX analysis. The particles were of multiply twinned structure, containing Pd–Au alloy particles with the similar Pd to Au ratio and coherent crystalline structure.

The changed interatomic distance on the surface could have both geometric and electronic effects on the catalytic behaviours. The results reported here are significant and highly interesting since bimetallic systems are widely used as catalysts in important fields such as fuel cells and electrocatalysis.

The synthesis of single-phase bimetallic catalysts is a promising way to improve the applicability of such catalysts for technical applications with high efficiency and performance.

## Notes and references


1 M. Haruta, T. Kobayashi, H. Sano and N. Yamada, *Chem. Lett.*, 1987, **4**, 405.
2 M. Valden, X. Lai and D. W. Goodman, *Science*, 1998, **281**, 1647.
3 P. Landon, P. J. Collier, A. F. Carley, D. Chadwick, A. J. Papworth, A. Burrows, C. J. Kiely and G. J. Hutchings, *Phys. Chem. Chem. Phys.*, 2003, **5**, 1917.
4 F. Porta, L. Prati, M. Rossi and G. Scari, *J. Catal.*, 2002, **211**, 464.
5 S. Carrettin, P. McMorn, P. Johnston, K. Griffin and G. J. Hutchings, *Chem. Commun.*, 2002, 696.
6 G. C. Bond and D. T. Thompson, *Catal. Rev. Sci. Eng.*, 1999, **41**, 319.
7 M. D. Hughes, Y. J. Xu, P. Jenkins, P. McMorn, P. Landon, D. I. Enache, A. F. Carley, G. A. Attard, G. J. Hutchings, F. King, E. Hugh Stitt, P. Johnston, K. Griffin and C. J. Kiely, *Nature*, 2005, **437**, 1132.
8 D. I. Enache, D. W. Knight and G. J. Hutchings, *Catal. Lett.*, 2005, **103**, 43.
9 L. Guczi, *Catal. Today*, 2005, **10**, 53 and reference cited therein.
10 C. L. Bianchi, P. Canton, N. Dimitratos, F. Porta and L. Prati, *Catal. Today*, 2005, **102**, 203.
11 N. Dimitratos, F. Porta, L. Prati and A. Villa, *Catal. Lett.*, 2005, **9**, 181.
12 M. Besson and P. Gallezot, *Catal. Today*, 2000, **57**, 127.
13 T. Mallat and A. Baiker, *Catal. Today*, 1994, **19**, 247 and reference cited therein.
14 C. Lemire, R. Meyer, S. Shaikhutdinov and H. J. Freund, *Angew. Chem., Int. Ed.*, 2004, **43**, 118.
15 M. Chen, D. Kumar, C. W. Yi and D. W. Goodman, *Science*, 2005, **310**, 291.
16 B. Gleich, M. Ruff and R. J. Behm, *Surf. Sci.*, 1997, **386**, 48.
17 L. Prati and F. Porta, *J. Catal.*, 2004, **224**, 397.
18 J. Van Gerpen, *Fuel Process. Technol.*, 2005, **86**, 1097.
19 A. M. Venezia, V. La Parola, V. Nicoli and G. Deganello, *J. Catal.*, 2002, **212**, 56.
20 J. L. Rodriguez-Lopez, J. M. Montejano-Carrizales, U. Pal, J. F. Sanchez-Ramirez, H. E. Troiani, D. Garcia, M. Miki-Yoshida and M. Jose-Yacaman, *Phys. Rev. Lett.*, 2004, **92**, 196102.
21 L. D. Marks, *Rep. Prog. Phys.*, 1994, **57**, 603.
22 H. Hofmeister, *Cryst. Res. Technol.*, 1998, **33**, 3.
23 L. A. Kibler, A. M. El-Aziz, R. Hoyer and D. M. Kolb, *Angew. Chem., Int. Ed.*, 2005, **44**, 2080.


 